An atomic charge model for graphene oxide for exploring its bioadhesive properties in explicit water

D. Stauffer,[1,2] N. Dragneva,[1,2] W. B. Floriano,[1,2] R. C. Mawhinney,[2] G. Fanchini,[3] S. French,[4] and O. Rubel[1,2]
[1]*Thunder Bay Regional Research Institute, 290 Munro St, Thunder Bay, Ontario P7B 6V4, Canada*
[2]*Lakehead University, 955 Oliver Road, Thunder Bay, Ontario P7A 7T1, Canada*
[3]*Physics and Astronomy, University of Western Ontario, 1151 Richmond St, London, Ontario N6A 3K7, Canada*
[4]*University of Calgary, South Health Campus, 4448 Front St. SE, Calgary, Alberta T3M 1M4, Canada*

(Received 24 April 2014; accepted 7 July 2014; published online 24 July 2014)

Graphene Oxide (GO) has been shown to exhibit properties that are useful in applications such as biomedical imaging, biological sensors, and drug delivery. The binding properties of biomolecules at the surface of GO can provide insight into the potential biocompatibility of GO. Here we assess the intrinsic affinity of amino acids to GO by simulating their adsorption onto a GO surface. The simulation is done using Amber03 force-field molecular dynamics in explicit water. The emphasis is placed on developing an atomic charge model for GO. The adsorption energies are computed using atomic charges obtained from an *ab initio* electrostatic potential based method. The charges reported here are suitable for simulating peptide adsorption to GO. © *2014 AIP Publishing LLC*. [http://dx.doi.org/10.1063/1.4890503]

I. INTRODUCTION

Properties of carbon-based nanomaterials in the context of biomedical applications continue to be a subject of extensive research due to the biocompatibility of these materials after functionalization.[1] Graphene-oxide (GO)—or graphene functionalized with epoxy, hydroxyl, and carboxyl groups—has been shown to exhibit properties that are useful in applications such as biomedical imaging, biological sensors, drug delivery, and biocompatible platforms for cell transfer and growth.[2–4] However, there is evidence of toxicity in cell-based as well as animal model studies.[2,5,6] The ability of GO to trigger adverse reactions when in contact with living tissue remains poorly understood.[3] In order to better assess the potential of GO in biomedical applications, it is useful to investigate its interactions with biomolecules.

Experimental studies report favorable adsorption of individual amino acids, peptides, proteins, and more complex biomolecules on the surface of GO.[7–10] The adsorption of seven peptides, ranging from 8 to 20 amino acids, to a GO surface was studied experimentally[9] by determining the concentration change in a solution before and after incubation with GO. Out of seven peptides tested, all except two exhibited a high adsorption ratio. This behavior is in line with the definition of bioadhesion proposed by Woodley *et al.*:[11] "Bioadhesion means the adherence of molecules (bioadhesives) to biological surfaces … bioadhesion does not normally involve the material forming covalent bonds with its target." Another evidence of GO-biomolecules interactions is provided by studying the quenching of an intrinsic fluorescence of isolated amino acids (tryptophan and tyrosine), peptides (amyloid peptide 40 ($A\beta_{40}$) and human islet amyloid polypeptide (hIAPP)), and proteins (Bovine serum albumin (BSA), and human serum albumin (HSA)).[12] The observed quenching indicates binding interactions between GO and free amino acids Trp and Tyr, the 40 amino acids $A\beta_{40}$ (one Tyr, no Trp), the 37 amino acids hIAPP (one Tyr, no Trp), BSA (two Trp), and HSA (one Trp). It was suggested that the quenching effect could result from $\pi - \pi$ interactions between Trp/Tyr and GO, similar to what is observed for Trp adsorption to graphene,[13] and/or to changes in peptide/protein conformation induced by the GO surface.

The molecular interactions of proteins with synthetic surfaces is a first step in the process of the integration of biomaterials with tissue.[14] Since amino acids are the building blocks of proteins, understanding their individual behavior on the surface can lead to a better understanding of the protein-surface interactions, and may aid the development of strategies for investigating those interactions. Recent studies showed progress in modeling the adsorption of amino acids and peptides to graphene surfaces such as carbon nanotubes,[13] boron-doped carbon nanotubes,[15] as well as calcium and hydrogen-doped graphene.[16] To the best of our knowledge, the only available data examining the binding of individual amino acids to GO are from an experimental study in which a mixture of all 20 amino acids was incubated with GO, and the concentration changes of each amino acid were assessed before and after incubation.[9] In this work, we simulate the adsorption of amino acids to GO in order to analyze its potential biocompatibility.

However, a difficulty in the modeling of GO is related to the ambiguity of its structure. Several models for the atomic structure of single hydroxyl or epoxy functional groups on the surface of GO have been proposed in the literature. These models include well-established parameters such as bond distances and angles[17–19] as well as the density and spacial distribution of the functional groups.[20] In addition to the structure, it is also important to provide atomic charges that most

accurately represent a GO surface in order to capture the electrostatic contributions to the interaction energy. The present work focuses on identifying an atomic charge model for GO that will provide the most consistent description for studying the interaction between GO and biomolecules in their natural environment (water). First, we discuss a method for the development of a charge model for GO based on analysis of the electrostatic potential (ESP). In the second part of the work, we report the results of simulations of the adsorption of the 20 proteinogenic amino acids onto the surface of GO using the atomic charges developed in this study. Simulations are performed using a force-field molecular dynamics approach in an explicit aqueous environment. The obtained adsorption energies are in line with the only available experimental data[9] and consistent with other theoretically computed results.[21,22] We show that the binding affinity of amino acids to the GO surface is slightly greater than to a pristine graphene surface. These results indicate that GO and graphene may exhibit similar bioadhesive characteristics.

II. METHOD

A. First principle calculation of electrostatic potential

A layer of GO was constructed with 60 carbon atoms arranged in a honeycomb pattern using an experimental value for the nearest-neighbor distance of 1.418 Å,[23] resulting in a 12.280 × 12.762 Å^2 block. Single epoxy and hydroxyl functional groups were placed at the surface as illustrated in Fig. 1. Periodic boundary conditions were applied in all three directions. GO layers were separated in the z-direction by adding a vacuum of 16 Å.

The electronic structure calculations were performed in the framework of density functional theory (DFT) implemented in the ABINIT package.[24,25] A plane wave basis set with a cutoff energy of 30 Ha was used in conjunction with Troullier-Martins pseudopotentials.[26] Perdew-Burke-Ernzerhof generalized gradient approximation was employed for the exchange-correlation functional.[27] The reciprocal space was sampled with a single k-point. A special distribution of the electrostatic potential was obtained by subtracting the exchange-correlation potential from the total Kohn-Sham potential. To confirm the completeness of the chosen basis set, a convergence test was performed for the water molecule in vacuum by computing its geometry, the electrostatic potential in the vicinity of the molecule, and the dipole moment. Less than 1% variation was observed when comparing the characteristics obtained using cutoff energies of 30 and 50 Ha.

The full relaxation of internal degrees of freedom was performed by minimizing the Hellmann-Feynman forces acting on individual atoms below 5 × 10^{-4} Ha/Bohr. The obtained structure and geometry of the functional groups on the GO surface is consistent with *ab initio* calculations reported in Refs. 18 and 28.

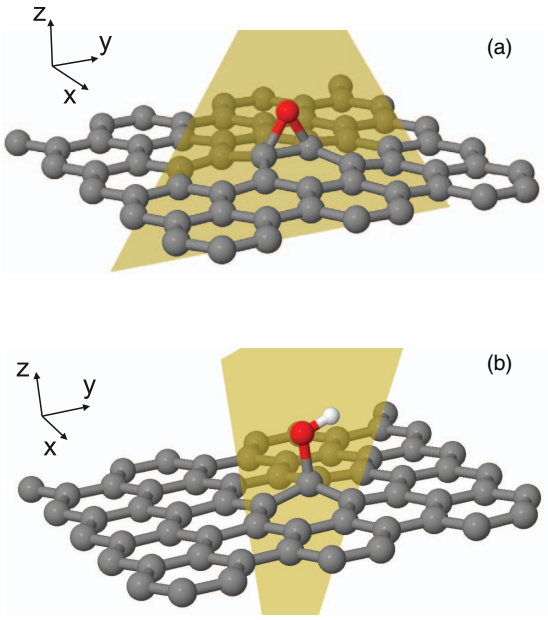

FIG. 1. Structural model of (a) epoxy and (b) hydroxyl functional groups at the surface of graphene used to determine point charges. Calculations of the electrostatic potential were performed within the yellow plane passing through the centres of C–O–C and C–O–H atoms in the case of epoxy and hydroxyl functional groups, respectively.

B. Point charge model

The point charges for the functional groups of the GO surface were chosen to reproduce the ESP calculated with DFT. This approach is known in the literature as the ESP charge model.[29–36] The Coulomb potential was calculated at grid points with a spacing of 0.05 Å on a two-dimensional plane constructed as shown in Fig. 1. The electrostatic potential at point $\mathbf{r}$ due to a point charge distribution is evaluated as

$$V(\mathbf{r}) = \sum_i \frac{q_i}{4\pi\varepsilon_0|\mathbf{R}_i - \mathbf{r}|}, \quad (1)$$

where ε_0 is the permittivity of free space, q_i and $\mathbf{R}_i$ are the point charge and the position vector of atom i, respectively.

A least-squares algorithm was employed to determine a set of charges that most accurately reproduces the ESP within a region of interest.[37,38] The region of interest included grid points located at a distance of $1.5 \le R \le 5$ Å from atoms in the functional group as well as bonded carbon atoms (Fig. 2). The lower bound excluded points within the van der Waals radius of each functional group atom.[34] It was also the shortest distance for non-bonded interactions between the atoms of the amino acid and of the GO surface observed in our simulations. The upper bound was the distance beyond which the Coulomb potential of the functional group was less than 0.01 Ry/e.[39] The zero net charge imposed an additional constraint $\sum_i q_i = 0$. Atomic charges were assigned only to atoms in a functional group and carbon atoms directly bonded to the functional group. Other neighbouring carbon atoms were given no charge, as it was found by Li *et al.*[40] that the charge is mostly localized at the carbon atoms bridged to the oxygen atom. We assume that the charge values of functional groups do not affect the charge values of neighboring functional groups.[41,42] The difference in charges for the functional groups obtained with the two-dimensional model and with a three-dimensional model was less than 5%. This difference can be considered negligible for the purpose of our simulations. An identical

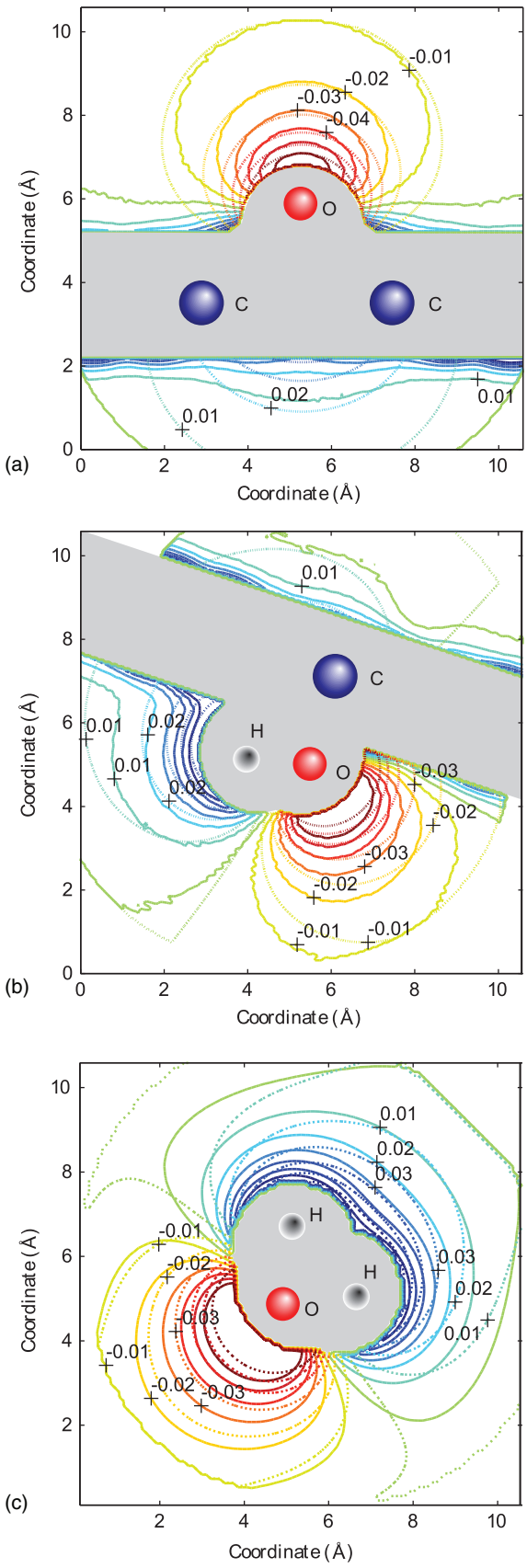

FIG. 2. Electrostatic potential (Ry/*e*) calculated with DFT (solid contours) and obtained from the ESP point charge model (dashed contours). The panels refer to (a) epoxy and (b) hydroxyl functional groups as well as (c) water molecule. Contour lines are shown within the region of interest discussed in the text. The shaded area depicts the excluded region with the proximity of less than 1.5 Å to atoms.

procedure was used to calculate ESP point charges for a single water molecule in vacuum.

All ESP charges were then scaled up by a factor of 1.5 in order to match the charges of the TIP3P water model (see Sec. III A), which is included in the Amber03 force-field and accurately reproduces the dipole moment as well as other thermodynamic properties of water.[43–45] This method was originally introduced in Ref. 30. The charge correction accounts for the polarization effect of an aqueous environment,[29,30,33,44] which leads to an increase in the experimental dipole moment of liquid water as compared to its gaseous state.[33,46] It is the scaled charge model (abbreviated as SESP) that will be used later in the modeling of GO.

C. Graphene oxide structure

The GO structure used in the molecular dynamics simulation was a 38×50 Å^2 section of graphene functionalized with epoxy and hydroxyl groups. The model consisted of a lattice of 768 carbon atoms with 96 hydroxyl and 60 epoxy groups distributed on both sides of the surface. A carbon to oxygen atom ratio of 5:1 and a hydroxyl to epoxy group ratio of 3:2 was chosen in accordance with the GO model proposed by Bagri *et al.*[20] The spatial distribution of the functional groups was also taken from Bagri *et al.*[20] The GO surface was built by repeating the unit cell shown in Fig. 3. The initial geometry for the functional groups was based on the works of Yan and Chou[28] and Xu and Xue.[18] The bond distance between carbon atoms was initially set at 1.418 Å (Fig. 3). In the hydroxyl group, the initial C–O bond length was 1.47 Å, the O–H bond length was 0.98 Å, and the C–O–H bond angle was 107.9°. For the epoxy group, the C–O bond distance was 1.44 Å, and the C–O–C bond angle was 63.9°.

D. Molecular dynamics simulation

GO and each of the 20 proteinogenic amino acids were placed in a simulation cell with dimensions of $38 \times 50 \times 60$ Å^3. Periodic boundary conditions were applied in all directions. Each amino acid was placed on the GO surface and the resulting system was energy-minimized in vacuum. This minimized structure was solvated with explicit water and used as the starting configuration for molecular dynamics simulations. To mimic the behavior of the amino acids as a part of a peptide chain, the ends of the amino acids were terminated with acetyl and methyl groups, which is a recently proposed procedure for modeling amino acids.[47,48] All 20 amino acids were consecutively placed on the top of GO with the longest axis parallel to the surface because this arrangement was found to be energetically more favorable.[49] Molecular dynamics NPT calculations were performed using the Amber03 force field[50] and the TIP3P water model[51] as implemented in the YASARA package.[52]

The simulations were carried out using the same methodology as in our previous study.[48] The simulation time for molecular dynamics was 40 ns, which is sufficiently long to achieve equilibrium as determined by stable values for the potential energy of the amino-acid–GO system. The simulations were performed using physiological parameters,

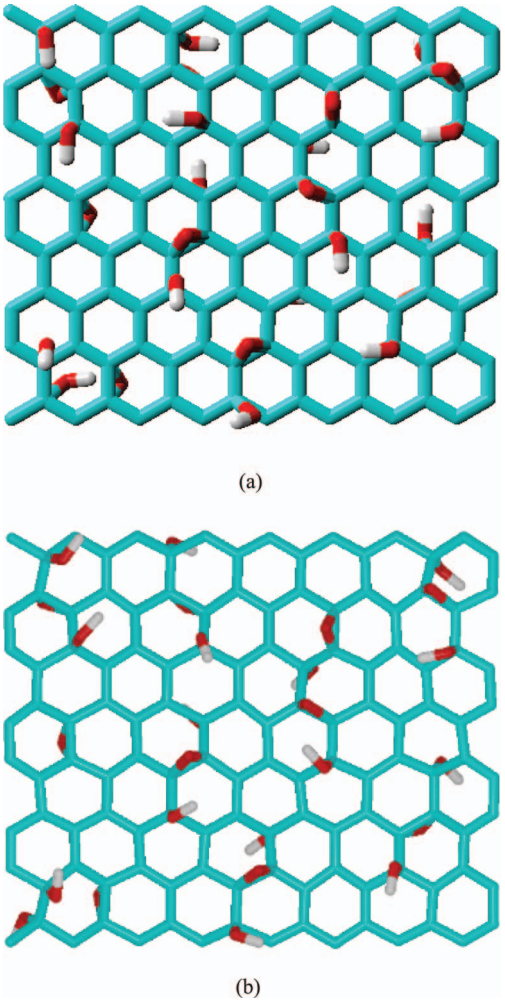

FIG. 3. The unit cell of the GO surface used for the simulation (a) before and (b) after minimization. The carbon atoms are shown in blue, the oxygen atoms in red, and the hydrogen atoms in white. After minimization, the cell shows some distortion due to the lengthening of the bond between the carbon atoms bound to the epoxy groups. The positively charged hydrogen atoms in the hydroxyl groups cause them to orient towards the negatively charged epoxy groups.

such as 1 atm. pressure, body temperature (310 K), and the standard sodium chloride concentration of blood (0.9%).

In the calculations that represent the bound state of the amino acids to GO, the carbon-α atom of the amino acid was initially placed 3–4 Å above the GO sheet and then the whole amino-acid–GO system was allowed to relax freely. The unbound state is represented by the corresponding amino acid and GO each simulated individually in the same environment and under the same conditions as the bound state. The adsorption energy was calculated as the difference between the sum of the potential energies of the amino acid and GO in the bound and unbound states, respectively,

$$E_{\text{ads}} = \langle E_{\text{a.a.}} + E_{\text{GO}} \rangle_{\text{bound}} - \langle E_{\text{a.a.}} \rangle_{\text{unbound}} - \langle E_{\text{GO}} \rangle_{\text{unbound.}} \tag{2}$$

Here, the individual energies of the amino acid and GO include their interactions with the surrounding environment (solvent and counterions). The angle brackets $\langle \dots \rangle$ represent time averaged values obtained with the same method as in our previous study.[48]

The adsorption energies were sensitive (up to 10% variation) to the initial position of the amino acid with respect to the GO surface. Therefore, a minimum of three simulations, corresponding to different starting configurations, were performed for each amino acid. The average of the adsorption energies of each amino acid over multiple simulations was calculated. Additional simulations were performed when needed to reduce the variation of the average adsorption energy to less than 0.05 eV.

III. RESULTS

A. Atomic point charge model for graphene oxide

Since molecular dynamics simulations are strongly influenced by the choice of atomic point charges,[53] we present a rigorous method for determining the partial charges of GO. The point charges calculated from *ab initio* electrostatic potential (ESP) are summarized in Table I along with the results obtained using alternative methods. The atomic charge of $-0.56e$ for the oxygen atom was found to best reproduce the electrostatic potential in the vicinity of the water molecule. The point charge for oxygen in the hydroxyl group has a lower value of $-0.38e$ in comparison to that in water. This result can be attributed to the higher electronegativity of carbon in comparison to hydrogen. For the same reason, the charge of oxygen in the epoxy group is even weaker ($-0.24e$).

It should be noted that the point charge obtained for oxygen in water is about 15% weaker than other *ab initio* ESP charges reported in the literature[54] (see Table I). In order to elucidate the reason, we computed the dipole moment of a water molecule using the *ab initio* electron density (not the point charges) in the framework of the modern theory of polarization (Berry phase).[55] The resulting dipole moment of 1.83 D agrees well with the experimental value of 1.86 D for a water molecule in the gas phase,[56] which gives us confidence in the calculated electron density and resulting potential. The discrepancy between *ab initio* ESP charges may therefore be attributed to differences in the definition of the region of interest and the distribution of sampling points (Sec. II B).

TABLE I. Partial charges (in units of the elementary charge) for the water molecule as well as epoxy and hydroxyl groups of GO determined using various charge models.

		Charge model			
Functional group or molecule	Atom	ESP (this work)	SESP (this work)	RESP[a]	Modified AM1-BCC[b]
Water molecule	O	−0.56	−0.84	−0.68	−0.834
	H	+0.28	+0.42	+0.34	+0.417
Epoxy	O	−0.24	−0.36	⋯	−0.36
	C	+0.12	+0.18	⋯	+0.18
Hydroxyl	O	−0.38	−0.57	⋯	−0.58
	C	+0.12	+0.18	⋯	+0.16
	H	+0.26	+0.39	⋯	+0.42

[a]Based on *ab initio* (MP2/aug-cc-pV6Z) electrostatic potential in conjunction with the RESP algorithm (Ref. 54).
[b]AM1-BCC charges corrected with known RESP charges for related functional groups Refs. 57 and 58.

In molecular dynamics simulations of molecular adsorption at the solid-liquid interface, solute-solvent and substrate-solvent interactions play an important role.[59,60] Therefore, special care should be taken in choosing a *mutually compatible* charge model for both solute and solvent. The YASARA software package with the Amber03 force field was chosen for the simulations because of its accuracy in modeling organic molecules in an aqueous environment.[61] This force field uses the TIP3P water model, which is a non-polarizable three-point water model.[51] The partial charges are fixed at the value of $-0.834e$ for the oxygen atom (Table I) and are not affected by proximity to other molecules.[29] The increase in the charge value relative to the gas phase is due to the polarization effect present in liquid water, which is implicitly included in the TIP3P model.[33] However, the ESP-derived charges for GO do not account for the charge increase due to polarization, which leads to an underestimation of the strength of the electrostatic interactions at the solute-solvent interface.[44]

This inconsistency can be resolved by the use of linearly scaled atomic point charges. The ESP-charges calculated in our work were scaled by a factor of 1.5 in order to match the charges on the TIP3P water model. The scaling factor is the ratio of the atomic charge on the oxygen atom of the TIP3P model ($-0.834e$) to the atomic charge for the oxygen atom in a water molecule calculated by the method described above ($-0.56e$). The scaled charges are listed in Table I under the SESP charge model. The scaling accounts for the additional polarization induced by the aqueous solution and ensures compatibility of the SESP atomic charges with the TIP3P water model. The polarization effects are also implicitly built into the charges employed by the AMBER force field for parametrization of amino acids. By applying the uniform scaling factor, we essentially imply that identical elements with identical hybridization (e.g., hydrogen in water and in the hydroxyl group) exhibit identical atomic polarizability,[62] resulting in a similar dipolar enhancement produced by the polar solvent.

Finally, we ensure that the proposed charges for the GO surface are compatible with the charge model that is used in our simulation to assign partial charges in unparameterized substrates. For this parametrization, YASARA relies on an `autoSMILES` program that uses the AM1-BCC algorithm[57] combined with known RESP charges.[37] The use of AM1-BCC charges in conjunction with the TIP3P water model has been show to accurately reproduce experimental values for hydration free energies of certain compounds.[63] This approach also reproduces TIP3P charges for the water molecule (Table I). The atomic charges generated by the `autoSMILES` code are listed in Table I under "Modified AM1-BCC." Their close agreement with SESP atomic charges gives us confidence in the compatibility of the charge models employed for the solvent, solute, and surface in this study.

B. Adsorption of amino acids on graphene oxide

Once point charges were assigned to all functional groups, an energy minimization for the GO surface was performed in vacuum. After minimization, the surface had an undulating (sinusoidal) shape, which agrees with the model suggested by Tung *et al.*[64] This non-planar shape can be explained by the electrostatic interactions between the functional groups attached to the surface as well as the change in coordination, from sp^2 to sp^3, for the carbons attached to the functional groups.[65] The bond distances and angles of the functional groups remained in good agreement with values calculated with DFT.[9,18,66] By giving a three-dimensional computer-generated molecular model of GO and chemically converted graphene, the authors suggest that the removal of the $-$OH and $-$COOH functionalities upon reduction of GO restores the planar structure of the graphene surface.

Next, we simulated the adsorption of individual capped amino acids on the surface of GO in water. The corresponding average adsorption energies E_{ads} for each 20 capped amino acids obtained with the SESP charges are shown in Fig. 4. The average adsorption energy values are also presented in the table of the supplementary material.[67] Overall, the adsorption of all amino acids on the surface of GO was energetically favorable, which is indicative of bioadhesive properties of the GO substrate. The adsorption energies of the amino acids on GO are 25% stronger (on average) in comparison to their adsorption energies on graphene.[48]

In order to better understand the origin of bioadhesive properties of GO, we split E_{ads} into two components: solute $\langle E_{a.a.}\rangle_{bound} - \langle E_{a.a.}\rangle_{unbound}$ and surface $\langle E_{GO}\rangle_{bound} - \langle E_{GO}\rangle_{unbound}$ contributions. The adsorption of amino acids on GO is primarily driven by the favorable interaction energy of the solute with the surface and with the environment. The amino acid contributes more than half to the total

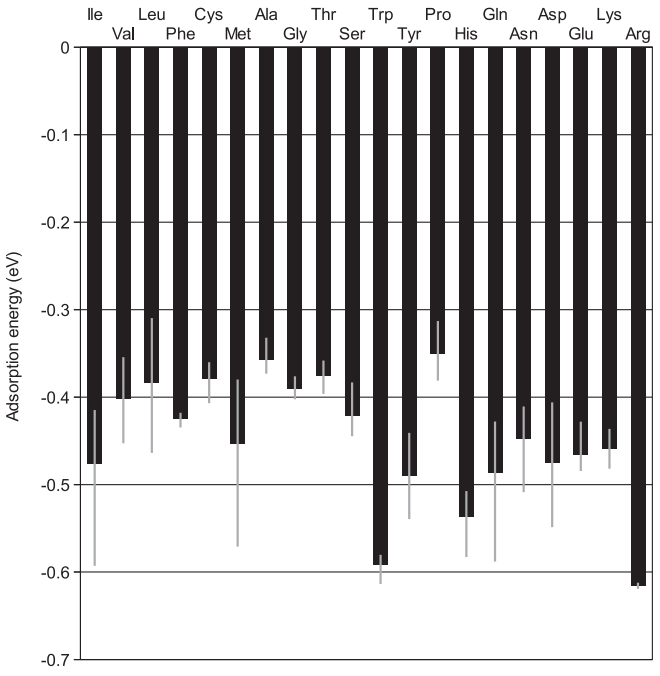

FIG. 4. Adsorption energies for 20 amino acids on the surface of GO calculated with the SESP charge model. The amino acids are arranged according to their hydropathy index. The data represent average values over multiple simulation runs with the gray error bars corresponding to minimum and maximum adsorption energies. In spite of the various adsorption strength, all amino acids remained bound to the surface within 99.7% of the simulation time.

binding energy, as it is shown in Fig. 1 of the supplementary material,[67] and defined by Eq. (2). Among various energy components (van der Waals, Coulomb, bond stretching, angle, dihedral, and planarity), the van der Waals contribution prevails in the adsorption energy (see Fig. 2 of the supplementary material.[67]). The van der Waals component correlates with the size of the amino acid: the larger the amino acid, the stronger the dispersion contribution to E_{ads}[22,48] (see Fig. 3 of the supplementary material[67]). In contrast, the Coulomb component, which can be attributed to the presence of polar groups at the GO surface as well as in the amino acids, favors solvation of amino acids, and disfavors their binding to the surface.

IV. DISCUSSION AND COMPARISON WITH EXPERIMENTS

Comparison of the binding affinity of amino acids to the GO surface with their binding affinity to other biomaterials could provide further insight into the potential biocompatibility of GO. Materials such as gold and hydroxyapatite have been used in medical and, particularly, in dental devices as coatings for biomedical implants.[21,22] According to Pan *et al.*,[21] B3LYP calculations show that glycine readily binds to hydroxyapatite in water. Our results also show that amino acids favor binding to the GO surface over remaining in water, indicating the potential for GO to exhibit bioadhesive features similar to hydroxyapatite. In another study, Feng *et al.*[22] calculated the adsorption energies of 20 amino acids to a gold surface with molecular dynamics using the CHARMM force field. The relative binding energies are similar to our results, with stronger energies for large amino acids, such as arginine, tryptophan, glutamine, methionine, asparagine, and tyrosine; and weaker energies for amino acids with smaller side chains, such as threonine, glycine, and alanine.[22] The similarities in the adsorption behavior of the amino acids to GO and to gold suggest similar bioadhesive characteristics for the two surfaces.

A. Adsorption of individual amino acids

Experimental literature reporting a quantitative evaluation of amino acid—GO interactions is scarce. To the best of our knowledge, the most comprehensive study was performed by Zhang *et al.*[9] The authors examined the binding of 20 uncapped amino acids to a GO surface by recording an adsorptive ratio, i.e., the ratio of the concentration of each amino acid in solution before and after incubation with the GO surface. A lower ratio for an individual amino acid indicates stronger binding to the GO surface.

Figure 5 shows the correlation between our calculated adsorption energies for uncapped amino acids and the experimental adsorptive ratios reported by Zhang *et al.*[9] The coefficient of determination for the linear regression fit to the data in Fig. 5 is $r^2 = 0.50$. This indicates that our model captures the general trend, i.e., stronger adsorption energies correspond to lower experimental adsorptive ratios. Approximately 50% of the variation in the data is not accounted for by the linear regression model. The experimental ratios for the 14 non-binding amino acids are close to 1, whereas the adsorption energies calculated for the corresponding amino acids in our simulations follow a continuous distribution. Comparison of the experimental adsorptive ratios and our adsorption energies is also effected by structural differences between the GO used experimentally by Zhang *et al.*[9] and the GO model in our simulations.

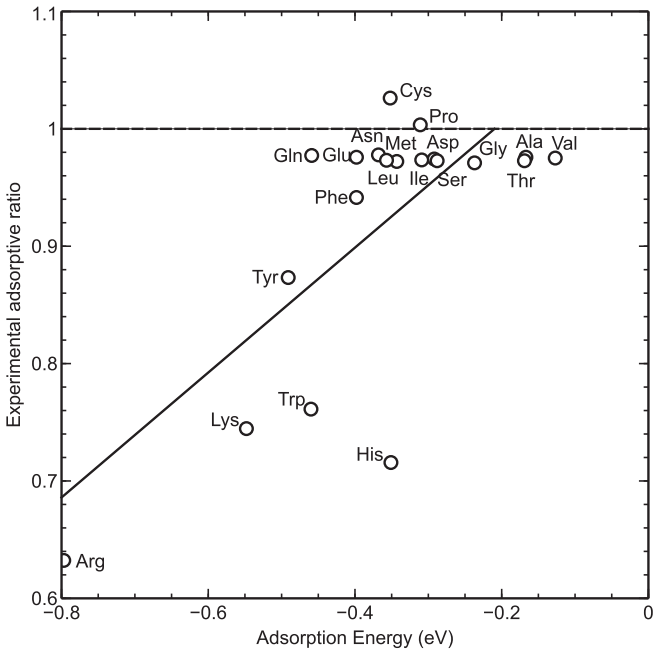

FIG. 5. Correlation of adsorption energies of uncapped amino acids at the surface of GO to the corresponding experimental adsorptive ratio.[9] Linear fit represents a general trend. The horizontal line shows the upper limit in the ratio of the non-bound amino acids according to experimental results.

The present work is focused on the modeling of a high-quality, idealized GO structure with epoxy and hydroxyl functional groups at the surface (Fig. 3). However, structural defects (such as vacancies) can be present in experimental GO samples as governed by specifics of the production technique.[68,69] In particular, carboxyl groups, which decorate the edges of GO fragments, can also be present near vacancies within the basal plane.[70] These carboxyl groups are negatively charged and, therefore, are highly reactive at physiological conditions. Experimentally,[9] positively charged amino acids (Arg and Lys) exhibit the highest affinity to GO surface followed by aromatic amino acids (Trp and Tyr). In our calculations, the protonated residues favorably interact with the epoxy and hydroxyl groups at the surface. The attractive electrostatic interaction with carboxyl groups present at defects and edges of the surface would contribute further to the favorable binding between GO and positively charged amino acids. GO-amino acid interactions are also influenced by the density of functional groups on the GO surface. The graphene oxide used in the experiment by Zhang *et al.*,[9] which was produced by the modified Hummer's method,[71] has a carbon to oxygen atomic ratio of 1.78:1,[72] compared to a C:O atomic ratio of 5:1 in our GO structure.[20] By taking into account this difference in the density of functional groups, as well as the effects of charged edges and/or defects and the synergetic interactions of multiple types of amino acids present in the solution,

the agreement with experiment (Fig. 5) can potentially be improved.

The ability of biomelecules to cross-link carbon nanostructures is utilized for their self-assembling.[73] The strength of such a link can also be used as an indirect measure of substrate-biomolecule interaction. A recent experimental study by Ahn *et al.*[74] examines the gelation of single layer sheets of GO induced by various groups of amino acids, which provides a qualitative measure of amino acid—GO interactions. Among six amino acids (Arg, Gly, Asn, Asp, Cys, Trp) tested experimentally, only arginine induce gelation at pH = 7.5. It is arginine that shows the strongest affinity to GO surface among all 20 amino acids in our calculations (Fig. 4).

B. Interaction with peptides

The influence of defects on adsorption can be illustrated by the seven peptides studied in Ref. 9. Two out of the 7 peptides studied have negative net charges at physiological conditions, and both of them have worse adsorption than neutral or positively charged peptides. The observed weaker binding of negatively charged peptides is presumably related to the mutual electrostatic repulsion between the peptides and GO, which is also negatively charged due to defects as discussed above. One of these peptides (ELAGAPPEPA), with a net charge of −2 at pH 7, showed no significant adsorption onto GO, whereas another peptide (RRREEETEEE) with a net charge of −3 exhibited weak binding. Although the behavior of a peptide on a surface is a function not only of its composition but, especially, of the particular sequence the amino acids appear within the peptide, a simple composition analysis of these peptides may provide useful insights into their interactions with GO. Based on amino acid composition and using our calculated adsorption energies for a pristine GO, average adsorption energies per amino acid can be estimated. This rough estimate of peptide-GO interaction suggests that the second peptide interacts more strongly with the surface (average adsorption energy per amino acid of −0.50 eV/residue) than the first (−0.38 eV/residue), due to the presence of the positively charged amino acids (Arg, R) which exhibit strong interactions with GO in our calculations even in the absence of carboxyl defects.

V. CONCLUSIONS

We present an atomic charge model for GO based on the *ab initio* ESP of epoxy and hydroxyl functional groups at the surface of GO. The proposed charge model is tailored to the TIP3P water model and includes polarization effects. Molecular dynamics simulations with the Amber03 force field were performed in order to assess the adsorption capacity of GO. The adsorption energies for 20 proteinogenic amino acids on the surface of GO were calculated using the scaled ESP charge model proposed above. The scaled ESP charges lead to the stable adsorption of amino acids to the surface. The bioadhesive properties of GO are similar to that of gold, however they can be weakened due to the presence of defects. Experimental evidence for the binding affinity of peptides to GO supports our proposed charge model.

ACKNOWLEDGMENTS

The authors would like to thank Dr. E. Krieger for the help in the development of the model for graphene oxide. D.S. would like to acknowledge the NSERC "Undergraduate Student Research Award" program. N.D. and O.R. would like to acknowledge the financial support of the Natural Sciences and Engineering Research Council of Canada (NSERC) under a Discovery Grant Program (386018-2010). High performance computational facilities of Lakehead University were used in this work.

[1] C. Cha, S. R. Shin, N. Annabi, M. R. Dokmeci, and A. Khademhosseini, ACS Nano **7**, 2891 (2013).
[2] H. Y. Mao, S. Laurent, W. Chen, O. Akhavan, M. Imani, A. A. Ashkarran, and M. Mahmoudi, Chem. Rev. **113**, 3407 (2013).
[3] P. Thevenot, W. Hu, and L. Tang, Curr. Top. Med. Chem. **8**, 270 (2008).
[4] D. Depan, B. Girase, J. Shah, and R. Misra, Acta Biomater. **7**, 3432 (2012).
[5] X. Hu and Q. Zhou, Chem. Rev. **113**, 3815 (2013).
[6] K. Wang, J. Ruan, H. Song, J. Zhang, Y. Wo, S. Guo, and D. Cui, Nanoscale Res. Lett. **6**, 8 (2011).
[7] X. Sun, Z. Liu, K. Welsher, J. T. Robinson, A. Goodwin, S. Zaric, and H. Dai, Nano Res. **1**, 203 (2008).
[8] J. Zhang, F. Zhang, H. Yang, X. Huang, H. Liu, J. Zhang, and S. Guo, Langmuir **26**, 6083 (2010).
[9] M. Zhang, B.-C. Yin, X.-F. Wang, and B.-C. Ye, Chem. Commun. **47**, 2399 (2011).
[10] Y. Zhang, C. Wu, S. Guo, and J. Zhang, Nanotechnol. Rev. **2**, 119 (2013).
[11] J. Woodley, Clin. Pharmacokinet. **40**, 77 (2001).
[12] S. Li, A. N. Aphale, I. G. Macwan, P. K. Patra, W. G. Gonzalez, J. Miksovska, and R. M. Leblanc, ACS Appl. Mater. Interf. **4**, 7069 (2012).
[13] C. Rajesh, C. Majumder, H. Mizuseki, and Y. Kawazoe, J. Chem. Phys. **130**, 124911 (2009).
[14] J. J. Gray, Curr. Opin. Struct. Biol. **14**, 110 (2004).
[15] W. Sun and Y. Bu, J. Phys. Chem. **112**, 15442 (2008).
[16] C. Cazorla, Thin Solid Films **518**, 6951 (2010).
[17] K. A. Mkhoyan, A. W. Contryman, J. Silcox, D. A. Stewart, G. Eda, C. Mattevi, S. Miller, and M. Chhowalla, Nano Lett. **9**, 1058 (2009).
[18] Z. Xu and K. Xue, Nanotechnology **21**, 045704 (2010).
[19] M. Topsakal and S. Ciraci, Phys. Rev. B **86**, 205402 (2012).
[20] A. Bagri, C. Mattevi, M. Acik, Y. J. Chabal, M. Chhowalla, and V. B. Shenoy, Nat. Chem. **2**, 581 (2010).
[21] H. Pan, J. Tao, X. Xu, and R. Tang, Langmuir **23**, 8972 (2007).
[22] J. Feng, R. B. Pandey, R. J. Berry, B. L. Farmer, R. R. Naik, and H. Heinz, Soft Matter **7**, 2113 (2011).
[23] R. W. G. Wyckoff, *Crystal Structures* (Interscience Publishers, New York, 1963).
[24] X. Gonze, G. M. Rignanese, M. Verstraete, J. M. Beuken, Y. Pouillon, R. Caracas, F. Jollet, M. Torrent, G. Zerah, M. Mikami, P. Ghosez, M. Veithen, J. Y. Raty, V. Olevano, F. Bruneval, L. Reining, R. Godby, G. Onida, D. R. Hamann, and D. C. Allan, Zeit. Kristallogr. **220**, 558 (2005).
[25] X. Gonze, B. Amadon, P.-M. Anglade, J.-M. Beuken, F. Bottin, P. Boulanger, F. Bruneval, D. Caliste, R. Caracas, M. Cote, T. Deutsch, L. Genovese, P. Ghosez, M. Giantomassi, S. Goedecker, D. Hamann, P. Hermet, F. Jollet, G. Jomard, S. Leroux, M. Mancini, S. Mazevet, M. Oliveira, G. Onida, Y. Pouillon, T. Rangel, G.-M. Rignanese, D. Sangalli, R. Shaltaf, M. Torrent, M. Verstraete, G. Zerah, and J. Zwanziger, Comput. Phys. Commun. **180**, 2582 (2009).
[26] N. Troullier and J. L. Martins, Phys. Rev. B **43**, 1993 (1991).
[27] J. P. Perdew, K. Burke, and M. Ernzerhof, Phys. Rev. Lett. **77**, 3865 (1996).
[28] J.-A. Yan and M. Y. Chou, Phys. Rev. B **82**, 125403 (2010).
[29] Y. Mo and J. Gao, J. Phys. Chem. B **110**, 2976 (2006).
[30] I. V. Leontyev, M. V. Vener, I. V. Rostov, M. V. Basilevsky, and M. D. Newton, J. Chem. Phys. **119**, 8024 (2003).
[31] J. Gao, J. Phys. Chem. B **101**, 657 (1997).
[32] O. Guvench, S. S. Mallajosyula, E. P. Raman, E. Hatcher, K. Vanommeslaeghe, T. J. Foster, F. W. Jamison, and A. D. MacKerell, J. Chem. Theory Comput. **7**, 3162 (2011).
[33] I. V. Leontyev and A. A. Stuchebrukhov, J. Chem. Theory Comput. **6**, 3153 (2010).

[34]D.-L. Chen, A. C. Stern, B. Space, and J. K. Johnson, J. Phys. Chem. A **114**, 10225 (2010).
[35]A. A. Bliznyuk, A. P. Rendell, T. W. Allen, and S.-H. Chung, J. Phys. Chem. B **105**, 12674 (2001).
[36]P. E. Mason, E. Wernersson, and P. Jungwirth, J. Phys. Chem. B **116**, 8145 (2012).
[37]C. I. Bayly, P. Cieplak, W. Cornell, and P. A. Kollman, J. Phys. Chem. **97**, 10269 (1993).
[38]J. Zeng, L. Duan, J. Zhang, and Y. Mei, J. Comput. Chem. **34**, 847 (2013).
[39]R. Garemyr and A. Elofsson, Proteins **37**, 417 (1999).
[40]Y. Li, B. Pathak, J. Nisar, Z. Qian, and R. Ahuja, Europhys. Lett. **103**, 28007 (2013).
[41]Y. Liu and J. Wilcox, Environ. Sci. Technol. **46**, 1940 (2012).
[42]A. P. Smith, A. E. McKercher, and R. Mawhinney, J. Phys. Chem. A **115**, 12544 (2011).
[43]P. Mark and L. Nilsson, J. Phys. Chem. **105**, 9954 (2001).
[44]J. Gao and X. Xia, Science **258**, 631 (1992).
[45]M. Shirts and V. Pande, J. Chem. Phys. **122**, 134508 (2005).
[46]Y. Tu and A. Laaksonen, Phys. Rev. E **64**, 026703 (2001).
[47]R. B. Pandey, Z. Kuang, B. L. Farmer, S. S. Kim, and R. R. Naik, Soft Matter **8**, 9101 (2012).
[48]N. Dragneva, W. B. Floriano, D. Stauffer, R. C. Mawhinney, G. Fanchini, and O. Rubel, J. Chem. Phys. **139**, 174711 (2013).
[49]W. Qin, X. Li, W.-W. Bian, X.-J. Fan, and J.-Y. Qi, Biomaterials **31**, 1007 (2010).
[50]Y. Duan, C. Wu, S. Chowdhury, M. Lee, G. Xiongand, W. Zhang, R. Yang, P. Cieplak, R. Luo, T. Lee, J. Caldwell, J. Wang, and P. Kollman, J. Comput. Chem. **24**, 1999 (2003).
[51]W. L. Jorgensen, J. Chandrasekhar, J. D. Madura, R. W. Impey, and M. L. Klein, J. Chem. Phys. **79**, 926 (1983).
[52]E. Krieger, G. Koraimann, and G. Vriend, Proteins **47**, 393 (2002).
[53]H. Heinz and U. W. Suter, J. Phys. Chem. B **108**, 18341 (2004).
[54]F. Martin and H. Zipse, J. Comput. Chem. **26**, 97 (2005).
[55]R. King-Smith and D. Vanderbilt, Phys. Rev. B **47**, 1651 (1993).
[56]P. L. Silvestrelli and M. Parrinello, Phys. Rev. Lett. **82**, 3308 (1999).
[57]A. Jakalian, D. B. Jack, and C. I. Bayly, J. Comput. Chem. **23**, 1623 (2002).
[58]J. Wang, R. M. Wolf, J. W. Caldwell, P. A. Kollman, and D. A. Case, J. Comput. Chem. **25**, 1157 (2004).
[59]A. D. MacKerell, J. D. Bashford, J. M. R. L. Dunbrack, J. D. Evanseck, M. J. Field, S. Fischer, J. Gao, H. Guo, S. Ha, D. Joseph-McCarthy, L. Kuchnir, K. Kuczera, F. T. K. Lau, C. Mattos, S. Michnick, T. Ngo, D. T. Nguyen, B. Prodhom, W. E. Reiher, B. Roux, M. Schlenkrich, J. C. Smith, R. Stote, J. Straub, M. Watanabe, J. Wiorkiewicz-Kuczera, D. Yin, and M. Karplus, J. Phys. Chem. **102**, 3586 (1998).
[60]B. L. Woods and R. A. Walker, J. Phys. Chem. A **117**, 6224 (2013).
[61]W. D. Cornell, P. Cieplak, C. I. Bayly, I. R. Gould, K. M. Merz, D. M. Ferguson, D. C. Spellmeyer, T. Fox, J. W. Caldwell, and P. A. Kollman, J. Am. Chem. Soc. **117**, 5179 (1995).
[62]B. Thole, Chem. Phys. **59**, 341 (1981).
[63]D. L. Mobley, E. Dumont, J. D. Chodera, and K. A. Dill, J. Phys. Chem. B **111**, 2242 (2007).
[64]V. C. Tung, M. J. Allen, Y. Yang, and R. B. Kaner, Nat. Nanotechnol. **4**, 25 (2009).
[65]M. J. McAllister, J.-L. Li, D. H. Adamson, H. C. Schniepp, A. A. Abdala, J. Liu, M. Herrera-Alonso, D. L. Milius, R. Car, R. K. Prud'homme, and I. A. Aksay, Chem. Mater. **19**, 4396 (2007).
[66]N. Ghaderi and M. Peressi, J. Phys. Chem. C **114**, 21625 (2010).
[67]See supplementary material at http://dx.doi.org/10.1063/1.4890503 for the adsorption energies of capped and uncapped amino acids at the surface of Graphene Oxide.
[68]H. C. Schniepp, J.-L. Li, M. J. McAllister, H. Sai, M. Herrera-Alonso, D. H. Adamson, R. K. Prud'homme, R. Car, D. A. Saville, and I. A. Aksay, J. Phys. Chem. B **110**, 8535 (2006).
[69]D. R. Dreyer, S. Park, C. W. Bielawski, and R. S. Ruoff, Chem. Soc. Rev. **39**, 228 (2010).
[70]S. Radic, N. K. Geitner, R. Podila, P. C. Ke, and F. Ding, Sci. Rep. **3**, 2273 (2013).
[71]L. Shahriary and A. A. Athawale, Int. J. Energy Environ. Eng. **2**, 58 (2014).
[72]M. Hirata, T. Gotou, S. Horiuchi, M. Fujiwara, and M. Ohba, Carbon **42**, 2929 (2004).
[73]D. Yu and L. Dai, J. Phys. Chem. Lett. **1**, 467 (2010).
[74]H. Ahn, T. K. H. Choi, C. Yoon, K. Um, J. Nam, K. H. Ahn, and K. Lee, Carbon **71**, 229 (2014).